



Comparison of the full-discretization methods for milling stability analysis by using different high-order polynomials to interpolate both state term and delayed term

Zhenghu Yan¹ · Changfu Zhang¹ · Xinguang Jiang¹ · Baoji Ma¹

Received: 12 December 2019 / Accepted: 13 April 2020 / Published online: 17 May 2020
© Springer-Verlag London Ltd., part of Springer Nature 2020

Abstract

This paper compares different full-discretization methods for milling stability analysis by using different high-order polynomials to interpolate both state term and delayed term (HFDMs) from the aspects of accuracy and efficiency. The dynamic model of milling process with consideration of regeneration effect is described by time periodic delay-differential equation (DDE) in the state-space. Different high-order interpolation polynomials are used to approximate the state term and delayed term. The state transition matrix is obtained on the basis of direct integration scheme. The rates of convergence of different HFDMs are compared with those of the benchmark methods using different process parameter points, the results indicate that it is difficult to evaluate the accuracy of different HFDMs through the convergence rate analysis of limited process parameter points. Then, mean differences and variances between the referenced and predicted critical depths of cut are employed for accuracy analysis. The 3rd-2nd HFDM is, on the whole, proved to be more accurate than the other methods. The efficiencies of different HFDMs are also verified through time-consuming study for both single degree of freedom (1-DOF) and two degree of freedom (2-DOF) milling system. The 3rd-2nd HFDM is proved to be an efficient method by comparing with the other methods. Besides, the HFDMs are available for predicting the stability lobe diagrams under both large immersion condition and low immersion condition.

Keywords Milling stability · Full-discretization method · Interpolation polynomial · Rate of convergence

1 Introduction

Chatter is one kind of self-excited vibrations in the dynamic system of milling, which limits the productivity and surface finish of the products but often occurs during milling operations. Regenerative chatter refers to the unstable phenomenon that a wavy surface left behind by previous tooth is removed by current tooth [1]. It is one of the most common obstacles to achieve high performance milling operations. Apart from leading to poor surface quality, chatter may cause premature failure of tools and machine tools. Therefore, chatter avoidance is an important issue in the milling process. With the aim of acquiring precision surface and high productivity, chatter-

free parameters should be adopted for machining. Stability lobe diagram that describes the boundary between stable and unstable milling operations can be employed to select chatter-free parameters.

Considering regenerative effect, the dynamic milling system can be modeled by time periodic delay-differential equation (DDE). The stability lobe diagram can be obtained by solving the time periodic DDE. Until now, a number of attempts at chatter stability prediction have been reported. The famous zeroth-order approximation (ZOA) method, which is proposed by Altintas and Budak [2], is the most efficient method. In this method, the Fourier series components are used to approximate the time varying dynamic cutting force coefficients. The axial depth of cut and the spindle speed are described by using real and image part of the characteristic equation of the system in frequency domain. By scanning a range of frequencies where chatter vibrations occur, the chatter-free axial depth of cuts and spindle speeds can be directly calculated using ZOA method. However, this method cannot be used to predict the stability for low radial immersion

✉ Zhenghu Yan
yanzh@xatu.edu.cn

¹ School of Mechatronic Engineering, Xi'an Technological University, Xi'an 710021, China

conditions. In order to make the ZOA method applicable to the low radial immersion conditions, Merdol et al. [3] presented a multi-frequency method. In this method, higher order harmonics of the Fourier series expansion are used to approximate the dynamic cutting force coefficients. In the ZOA method and multi-frequency method, the nonlinear features of milling system are not taken into consideration. Regarding the nonlinear features of milling system, Balachandran et al. [4, 5] studied the nonlinear oscillations of milling operation. In their works, the multiple regenerative effect and loss-of-contact effect are considered for analyzing the stability in milling. Long et al. [6, 7] presented the milling-process models which take the feed-rate effect, loss-of-contact effect, and the time-delay effects associated with the chip thickness variation into consideration. Since the stability lobe diagrams obtained by using linear models are available for predicting the milling stability, most of the milling stability prediction methods are based on linear models.

The ZOA method and multi-frequency method are the analytical methods in frequency domain; many numerical methods in time domain are also proposed, including temporal finite element analysis method (TFEA) [8], semi-discretization method (SDM) [9], first order semi-discretization method (1stSDM) [10], Chebyshev collocation method [11], full-discretization method (FDM) [12], numerical integration method [13], differential quadrature method [14], complete discretization scheme (CDS) [15], Runge-Kutta-based methods [16], Runge-Kutta-based complete discretization method [17], improved complete discretization method (ICDM) [18], Simpson-based method [19], spectral element method [20], numerical differentiation method [21], Adams-Moulton-based method [22], second order semi-discretization method [23], improved precise integration method [24], and so on.

The full-discretization method (FDM) [12] proposed by Ding et al. is a well-known method. In this method, the state term, delayed term, and periodic coefficient matrixes are all approximated using linear interpolation. The efficiency of the FDM is proved to be good. Inspired by the FDM, many milling stability prediction methods have been put forward. Ding et al. [25] presented a second order FDM (2nd FDM) which employs second order interpolation polynomial to approximate the state term. Liu et al. [26] presented a Hermite interpolation-based FDM which employs the second order Hermite interpolation polynomial and second order Lagrange interpolation polynomial to approximate the state term and delayed term, respectively. Guo et al. [27] suggested a third order FDM (3rd FDM) by using third order Newton interpolation polynomial to interpolate the state term. Ozoegwu [28] reported a least squares approximation method which utilizes least squares method to approximate the state term, delayed term, and periodic coefficient matrix. Then, Ozoegwu et al. [29] reported the hyper-third order full-

discretization methods to predict the stability in milling. In their work, the fourth order FDM (4th FDM) is proved to be more accurate than the other order FDMs. Ji et al. [30] proposed the higher-order Hermite-Newton-based method for stability prediction in milling. Recently, Tang et al. [31] proposed a second order updated full-discretization method (2nd UFDM) to predict the stability in milling. In this method, the state term and delayed term are both interpolated by second order interpolation polynomials. After that, Yan et al. [32] presented a third order updated full-discretization method (3rd UFDM). In this method, the state term and delayed terms are both approximated by third order interpolation polynomials. Zhou et al. [33] presented a series of full-discretization methods by interpolating the delay term of time-delayed differential equations (DFDMs), i.e., 1st DFDM, 2nd DFDM, 3rd DFDM, and 4th DFDM, to predict the milling stability.

In the FDM, 2nd FDM, 3rd FDM, and 4th FDM, the state term is interpolated by different-order interpolation polynomials, while the delayed term is only interpolated by first order interpolation polynomial. Similarly, in the 1st DFDM, 2nd DFDM, 3rd DFDM, and 4th DFDM, different-order interpolation polynomials are employed to interpolate the delayed term, while only the first order interpolation polynomial is employed to interpolate the state term. Although in the 2nd UFDM and 3rd UFDM the state term and delayed term are both approximated by high-order interpolation polynomials, the interpolation polynomials used to approximate the state term and delayed term have the same order. The study on employing different high-order interpolation polynomials to interpolate the state term and delayed term is also worth carrying out. Besides, the accuracy and efficiency of the prediction methods are sensitive to the order of interpolation polynomials. Therefore, in this work, the full-discretization methods which employ different high-order interpolation polynomials to interpolate the state term and delayed term (HFDMs) are compared with the existing high-order full-discretization methods. The accuracy and the efficiency of different HFDMs are evaluated by using comparison results.

The rest of this paper is organized as below. In Section 2, the mathematical model of the proposed methods is described, and different order interpolation polynomials are used to interpolate the state term and delayed term. In Section 3, model verification is conducted; the proposed methods are verified from the aspects of accuracy and efficiency. Conclusions are drawn in Section 4.

2 Mathematical model

The milling dynamics with consideration of regenerative effect can be modeled by delay-differential equation in the state-space as [9].

$$\dot{\mathbf{x}}(t) = \mathbf{A}\mathbf{x}(t) + \mathbf{B}(t)\mathbf{x}(t) - \mathbf{B}(t)\mathbf{x}(t - \tau) \tag{1}$$

where $\mathbf{x}(t)$ is the state variable of the milling system, \mathbf{A} is a constant matrix, and $\mathbf{B}(t)$ is a periodic coefficient matrix with the period T , that is $\mathbf{B}(t) = \mathbf{B}(t + T)$.

To numerically solve Eq. (1) by employing direct integration scheme, firstly, the time period T is equally divided into n small time intervals with the length of h , that is, $T = nh$, where n is an integer. After that, Eq. (1) is integrated on the i th small time interval $[ih, (i + 1)h]$ resulting in

$$\mathbf{x}(t) = e^{\mathbf{A}(t-ih)}\mathbf{x}(ih) + \int_{ih}^t e^{\mathbf{A}(t-\xi)}(\mathbf{B}(\xi)\mathbf{x}(\xi) - \mathbf{B}(\xi)\mathbf{x}(\xi - \tau))d\xi \tag{2}$$

Equation (2) can be equivalently written as

$$\begin{aligned} \mathbf{x}(ih + h) &= e^{\mathbf{A}h}\mathbf{x}(ih) \\ &+ \int_0^h e^{\mathbf{A}\xi}(\mathbf{B}(ih + h - \xi)\mathbf{x}(ih + h - \xi) - \mathbf{B}(ih + h - \xi)\mathbf{x}(ih + h - \xi - \tau))d\xi \end{aligned} \tag{3}$$

In order to obtain the state transition matrix of the milling system, different order interpolation polynomials are used to approximate the state term $\mathbf{x}(ih + h - \xi)$ and delayed term $\mathbf{x}(ih + h - \xi - \tau)$, respectively. In the literature [29], it is indicated that highest accuracy of the full-discretization methods can be achieved when the state term is approximated by fourth order interpolation polynomial. Additionally, Zhou et al. [33] pointed out that the rise in accuracy and convergence rate of the DFDM nearly stopped when the interpolation order for delayed term was up to fourth order. According to the above analysis, it is indicated that there is no need to interpolate the state term and delayed term by hyper-fourth order interpolation polynomial.

In the following part of this work, when the second order interpolation polynomial is employed to interpolate both the state term and delayed term, it is named second-second high-order full-discretization method (2nd-2nd HFDm). When the second order interpolation polynomial is employed to interpolate the state term, and the third order interpolation polynomial is employed to interpolate the delayed term, it is named second-third high-order full-discretization method (2nd-3rd HFDm), the rest can be named in a similar way.

In the literature [31], it is pointed out that high-order interpolation of periodic coefficient matrix has no apparent effect on improving effectiveness and efficiency. Therefore, in this work, the periodic coefficient matrix $\mathbf{B}(ih + h - \xi)$ is interpolated by first order interpolation polynomial and written as

$$\mathbf{B}(ih + h - \xi) \approx \frac{\xi}{h}\mathbf{B}_i + \frac{(h - \xi)}{h}\mathbf{B}_{i+1} \tag{4}$$

2.1 Interpolation for state term

2.1.1 State term interpolated by second order interpolation polynomial

When the state term $\mathbf{x}(ih + h - \xi)$ is interpolated by second order interpolation polynomial, the nodal values $\mathbf{x}(ih - h)$, $\mathbf{x}(ih)$, and $\mathbf{x}(ih + h)$ denoted as \mathbf{x}_{i-1} , \mathbf{x}_i , and \mathbf{x}_{i+1} , respectively, are employed for interpolation. The state term $\mathbf{x}(ih + h - \xi)$ can be expressed as

$$\begin{aligned} \mathbf{x}(ih + h - \xi) &= \frac{\xi(\xi - h)}{2h^2}\mathbf{x}_{i-1} + \frac{\xi(2h - \xi)}{h^2}\mathbf{x}_i \\ &+ \frac{(h - \xi)(2h - \xi)}{2h^2}\mathbf{x}_{i+1} \end{aligned} \tag{5}$$

Combining Eqs. (4) and (5), the following result can be obtained using direct integration scheme

$$\begin{aligned} &\int_0^h e^{\mathbf{A}\xi}\mathbf{B}(ih + h - \xi)\mathbf{x}(ih + h - \xi)d\xi \\ &= \begin{pmatrix} (\mathbf{G}_{21}\mathbf{B}_{i+1} + \mathbf{G}_{22}\mathbf{B}_i)\mathbf{x}_{i-1} + (\mathbf{G}_{23}\mathbf{B}_{i+1} + \mathbf{G}_{24}\mathbf{B}_i)\mathbf{x}_i + \\ (\mathbf{G}_{25}\mathbf{B}_{i+1} + \mathbf{G}_{26}\mathbf{B}_i)\mathbf{x}_{i+1} \end{pmatrix} \end{aligned} \tag{6}$$

where

$$\begin{aligned} \mathbf{G}_{21} &= -\frac{\mathbf{F}_2}{2h} + \frac{\mathbf{F}_3}{h^2} - \frac{\mathbf{F}_4}{2h^3}, \quad \mathbf{G}_{22} = -\frac{\mathbf{F}_3}{2h^2} + \frac{\mathbf{F}_4}{2h^3} \\ \mathbf{G}_{23} &= \frac{2\mathbf{F}_2}{h} - \frac{3\mathbf{F}_3}{h^2} + \frac{\mathbf{F}_4}{h^3}, \quad \mathbf{G}_{24} = \frac{2\mathbf{F}_3}{h^2} - \frac{\mathbf{F}_4}{h^3} \\ \mathbf{G}_{25} &= \mathbf{F}_1 - \frac{5\mathbf{F}_2}{2h} + \frac{2\mathbf{F}_3}{h^2} - \frac{\mathbf{F}_4}{2h^3}, \quad \mathbf{G}_{26} = \frac{\mathbf{F}_2}{h} - \frac{3\mathbf{F}_3}{2h^2} + \frac{\mathbf{F}_4}{2h^3} \end{aligned} \tag{7}$$

where

$$\begin{aligned} \mathbf{F}_0 &= e^{\mathbf{A}h} \\ \mathbf{F}_1 &= \mathbf{A}^{-1}(\mathbf{F}_0 - \mathbf{I}) \\ \mathbf{F}_2 &= \mathbf{A}^{-1}(h\mathbf{F}_0 - \mathbf{F}_1) \\ \mathbf{F}_3 &= \mathbf{A}^{-1}(h^2\mathbf{F}_0 - 2\mathbf{F}_2) \\ \mathbf{F}_4 &= \mathbf{A}^{-1}(h^3\mathbf{F}_0 - 3\mathbf{F}_3) \end{aligned} \tag{8}$$

2.1.2 State term interpolated by third order interpolation polynomial

In this section, the state term $\mathbf{x}(ih + h - \xi)$ is interpolated by third order interpolation polynomial, the nodal values $\mathbf{x}(ih - 2h)$, $\mathbf{x}(ih - h)$, $\mathbf{x}(ih)$, and $\mathbf{x}(ih + h)$ denoted as \mathbf{x}_{i-2} , \mathbf{x}_{i-1} , \mathbf{x}_i , and \mathbf{x}_{i+1} , respectively, are employed for interpolation. The state term $\mathbf{x}(ih + h - \xi)$ can be expressed as

$$\begin{aligned} \mathbf{x}(ih + h - \xi) &= \left(\frac{\xi}{3h} - \frac{\xi^2}{2h^2} + \frac{\xi^3}{6h^3} \right) \mathbf{x}_{i-2} + \left(-\frac{3\xi}{2h} + \frac{2\xi^2}{h^2} - \frac{\xi^3}{2h^3} \right) \mathbf{x}_{i-1} \\ &\quad \left(\frac{3\xi}{h} - \frac{5\xi^2}{2h^2} + \frac{\xi^3}{2h^3} \right) \mathbf{x}_i + \left(1 - \frac{11\xi}{6h} + \frac{\xi^2}{h^2} - \frac{\xi^3}{6h^3} \right) \mathbf{x}_{i+1} \end{aligned} \quad (9)$$

Combining Eqs. (4) and (9), the following result can be obtained using direct integration scheme

$$\int_0^h e^{A\xi} \mathbf{B}(ih + h - \xi) \mathbf{x}(ih + h - \xi) d\xi = \left(\begin{array}{l} (\mathbf{G}_{31}\mathbf{B}_{i+1} + \mathbf{G}_{32}\mathbf{B}_i)\mathbf{x}_{i-2} + (\mathbf{G}_{33}\mathbf{B}_{i+1} + \mathbf{G}_{34}\mathbf{B}_i)\mathbf{x}_{i-1} + \\ (\mathbf{G}_{35}\mathbf{B}_{i+1} + \mathbf{G}_{36}\mathbf{B}_i)\mathbf{x}_i + (\mathbf{G}_{37}\mathbf{B}_{i+1} + \mathbf{G}_{38}\mathbf{B}_i)\mathbf{x}_{i+1} \end{array} \right) \quad (10)$$

where

$$\begin{aligned} \mathbf{G}_{31} &= \frac{F_2}{3h} - \frac{5F_3}{6h^2} + \frac{2F_4}{3h^3} - \frac{F_5}{6h^4}, \quad \mathbf{G}_{32} = \frac{F_3}{3h^2} - \frac{F_4}{2h^3} + \frac{F_5}{6h^4} \\ \mathbf{G}_{33} &= \frac{2h}{-3F_2} + \frac{2h^2}{7F_3} - \frac{2h^3}{5F_4} + \frac{2h^4}{F_5}, \quad \mathbf{G}_{34} = \frac{2h^2}{-3F_3} + \frac{2h^3}{2F_4} - \frac{2h^4}{F_5} \\ \mathbf{G}_{35} &= \frac{3F_2}{h} - \frac{11F_3}{2h^2} + \frac{3F_4}{h^3} - \frac{F_5}{2h^4}, \quad \mathbf{G}_{36} = \frac{3F_3}{h^2} - \frac{5F_4}{2h^3} + \frac{F_5}{2h^4} \\ \mathbf{G}_{37} &= F_1 - \frac{17F_2}{6h} + \frac{17F_3}{6h^2} - \frac{7F_4}{6h^3} + \frac{F_5}{6h^4}, \quad \mathbf{G}_{38} = \frac{F_2}{h} - \frac{11F_3}{6h^2} + \frac{F_4}{h^3} - \frac{F_5}{6h^4} \end{aligned} \quad (11)$$

$$\begin{aligned} \mathbf{x}(ih + h - \xi) &= \left(\frac{-\xi}{4h} + \frac{11\xi^2}{24h^2} - \frac{\xi^3}{4h^3} + \frac{\xi^4}{24h^4} \right) \mathbf{x}_{i-3} + \left(\frac{4\xi}{3h} - \frac{7\xi^2}{3h^2} + \frac{7\xi^3}{6h^3} - \frac{\xi^4}{6h^4} \right) \mathbf{x}_{i-2} + \left(-\frac{3\xi}{h} + \frac{19\xi^2}{4h^2} - \frac{2\xi^3}{h^3} + \frac{\xi^4}{4h^4} \right) \mathbf{x}_{i-1} \\ &\quad \left(\frac{4\xi}{h} - \frac{13\xi^2}{3h^2} + \frac{3\xi^3}{2h^3} - \frac{\xi^4}{6h^4} \right) \mathbf{x}_i + \left(1 - \frac{25\xi}{12h} + \frac{35\xi^2}{24h^2} - \frac{5\xi^3}{12h^3} + \frac{\xi^4}{24h^4} \right) \mathbf{x}_{i+1} \end{aligned} \quad (13)$$

Combining Eqs. (4) and (13), the following result can be obtained using direct integration scheme

$$\int_0^h e^{A\xi} \mathbf{B}(ih + h - \xi) \mathbf{x}(ih + h - \xi) d\xi = \left(\begin{array}{l} (\mathbf{G}_{41}\mathbf{B}_{i+1} + \mathbf{G}_{42}\mathbf{B}_i)\mathbf{x}_{i-3} + (\mathbf{G}_{43}\mathbf{B}_{i+1} + \mathbf{G}_{44}\mathbf{B}_i)\mathbf{x}_{i-2} + \\ (\mathbf{G}_{45}\mathbf{B}_{i+1} + \mathbf{G}_{46}\mathbf{B}_i)\mathbf{x}_{i-1} + (\mathbf{G}_{47}\mathbf{B}_{i+1} + \mathbf{G}_{48}\mathbf{B}_i)\mathbf{x}_i + \\ (\mathbf{G}_{49}\mathbf{B}_{i+1} + \mathbf{G}_{410}\mathbf{B}_i)\mathbf{x}_{i+1} \end{array} \right) \quad (14)$$

where

$$\begin{aligned} \mathbf{G}_{41} &= \frac{-F_2}{4h} + \frac{17F_3}{24h^2} - \frac{17F_4}{24h^3} + \frac{7F_5}{24h^4} - \frac{F_6}{24h^5}, \quad \mathbf{G}_{42} = \frac{-F_3}{4h^2} + \frac{11F_4}{24h^3} - \frac{F_5}{4h^4} + \frac{F_6}{24h^5} \\ \mathbf{G}_{43} &= \frac{4F_2}{3h} - \frac{11F_3}{3h^2} + \frac{7F_4}{2h^3} - \frac{4F_5}{3h^4} + \frac{F_6}{6h^5}, \quad \mathbf{G}_{44} = \frac{4F_3}{3h^2} - \frac{7F_4}{3h^3} + \frac{7F_5}{6h^4} - \frac{F_6}{6h^5} \\ \mathbf{G}_{45} &= -\frac{3F_2}{h} + \frac{31F_3}{4h^2} - \frac{27F_4}{4h^3} + \frac{9F_5}{4h^4} - \frac{F_6}{4h^5}, \quad \mathbf{G}_{46} = -\frac{3F_3}{h^2} + \frac{19F_4}{4h^3} - \frac{2F_5}{h^4} + \frac{F_6}{4h^5} \\ \mathbf{G}_{47} &= \frac{4F_2}{h} - \frac{25F_3}{3h^2} + \frac{35F_4}{6h^3} - \frac{5F_5}{6h^4} + \frac{F_6}{6h^5}, \quad \mathbf{G}_{48} = \frac{4F_3}{h^2} - \frac{13F_4}{3h^3} + \frac{3F_5}{2h^4} - \frac{F_6}{6h^5} \\ \mathbf{G}_{49} &= F_1 - \frac{37F_2}{12h} + \frac{85F_3}{24h^2} - \frac{15F_4}{8h^3} + \frac{11F_5}{24h^4} - \frac{F_6}{24h^5}, \quad \mathbf{G}_{410} = \frac{F_2}{h} - \frac{25F_3}{12h^2} + \frac{35F_4}{24h^3} - \frac{5F_5}{12h^4} + \frac{F_6}{24h^5} \end{aligned} \quad (15)$$

where

$$\mathbf{F}_5 = \mathbf{A}^{-1} (h^4 \mathbf{F}_0 - 4\mathbf{F}_4) \quad (12)$$

2.1.3 State term interpolated by fourth order interpolation polynomial

Here, the nodal values $\mathbf{x}(ih - 3h)$, $\mathbf{x}(ih - 2h)$, $\mathbf{x}(ih - h)$, $\mathbf{x}(ih)$, and $\mathbf{x}(ih + h)$ denoted as \mathbf{x}_{i-3} , \mathbf{x}_{i-2} , \mathbf{x}_{i-1} , \mathbf{x}_i , and \mathbf{x}_{i+1} , respectively, are employed to interpolate the state term $\mathbf{x}(ih + h - \xi)$ using fourth order interpolation polynomial. Then, the state term $\mathbf{x}(ih + h - \xi)$ can be expressed as

where

$$F_6 = A^{-1}(h^5 F_0 - 5F_4) \tag{16}$$

2.2 Interpolation for delayed term

2.2.1 Delayed term interpolated by second order interpolation polynomial

When the delayed term $x(ih + h - \xi - T)$ is interpolated by second order interpolation polynomial, the nodal values $x(ih + 2h - T)$, $x(ih + h - T)$, and $x(ih - T)$ denoted as x_{i-n+2} , x_{i-n+1} , and x_{i-n} are employed for interpolation. The delayed term $x(ih + h - \xi - T)$ can be expressed as

$$x(ih + h - \xi - T) = \frac{\xi(\xi - h)}{2h^2} x_{i+2-n} + \frac{(h - \xi)(h + \xi)}{2h^2} x_{i+1-n} + \frac{\xi(\xi + h)}{2h^2} x_{i-n} \tag{17}$$

Combining Eqs. (4) and (17), the following result can be obtained using direct integration scheme

$$\int_0^h e^{A\xi} B(ih + h - \xi)x(ih + h - \xi - T)d\xi = \left(\begin{matrix} (H_{21}B_{i+1} + H_{22}B_i)x_{i+2-n} + (H_{23}B_{i+1} + H_{24}B_i)x_{i+1-n} + \\ (H_{25}B_{i+1} + H_{26}B_i)x_{i-n} \end{matrix} \right) \tag{18}$$

where

$$\begin{aligned} H_{21} &= -\frac{F_2}{2h} + \frac{F_3}{h^2} - \frac{F_4}{2h^3}, H_{22} = -\frac{F_3}{2h^2} + \frac{F_4}{2h^3} \\ H_{23} &= F_1 - \frac{F_2}{h} - \frac{F_3}{h^2} + \frac{F_4}{h^3}, H_{24} = \frac{F_2}{h} - \frac{F_4}{h^3} \\ H_{25} &= \frac{F_2}{2h} - \frac{F_4}{2h^3}, H_{26} = \frac{F_3}{2h^2} + \frac{F_4}{2h^3} \end{aligned} \tag{19}$$

2.2.2 Delayed term interpolated by third order interpolation polynomial

When the delayed term $x(ih + h - \xi - T)$ is interpolated by third order interpolation polynomial, the nodal values $x(ih +$

$3h - T)$, $x(ih + 2h - T)$, $x(ih + h - T)$, and $x(ih - T)$ denoted as x_{i-n+3} , x_{i-n+2} , x_{i-n+1} , and x_{i-n} are employed for interpolation. The delayed term $x(ih + h - \xi - T)$ can be expressed as

$$x(ih + h - \xi - T) = \left(\frac{\xi}{6h} - \frac{\xi^3}{6h^3} \right) x_{i+3-n} + \left(\frac{-\xi}{h} + \frac{\xi^2}{2h^2} + \frac{\xi^3}{2h^3} \right) x_{i+2-n} + \left(1 + \frac{\xi}{2h} - \frac{\xi^2}{h^2} - \frac{\xi^3}{2h^3} \right) x_{i+1-n} + \left(\frac{\xi}{3h} + \frac{\xi^2}{2h^2} + \frac{\xi^3}{6h^3} \right) x_{i-n} \tag{20}$$

Combining Eqs. (4) and (20), the following result can be obtained using direct integration scheme

$$\int_0^h e^{A\xi} B(ih + h - \xi)x(ih + h - \xi - T)d\xi = \left(\begin{matrix} (H_{31}B_{i+1} + H_{32}B_i)x_{i+3-n} + (H_{33}B_{i+1} + H_{34}B_i)x_{i+2-n} + \\ (H_{35}B_{i+1} + H_{36}B_i)x_{i+1-n} + (H_{37}B_{i+1} + H_{38}B_i)x_{i-n} \end{matrix} \right) \tag{21}$$

where

$$\begin{aligned} H_{31} &= \frac{F_2}{6h} - \frac{F_3}{6h^2} - \frac{F_4}{6h^3} + \frac{F_5}{6h^4}, H_{32} = \frac{F_3}{6h^2} - \frac{F_5}{6h^4} \\ H_{33} &= \frac{-F_2}{h} + \frac{3F_3}{2h^2} - \frac{F_5}{2h^4}, H_{34} = \frac{-F_3}{h^2} + \frac{F_4}{2h^3} + \frac{F_5}{2h^4} \\ H_{35} &= F_1 - \frac{F_2}{2h} - \frac{3F_3}{2h^2} + \frac{F_4}{2h^3} + \frac{F_5}{2h^4}, H_{36} = \frac{F_2}{h} + \frac{F_3}{2h^2} - \frac{F_4}{h^3} - \frac{F_5}{2h^4} \\ H_{37} &= \frac{F_2}{3h} + \frac{F_3}{6h^2} - \frac{F_4}{3h^3} - \frac{F_5}{6h^4}, H_{38} = \frac{F_3}{3h^2} + \frac{F_4}{2h^3} + \frac{F_5}{6h^4} \end{aligned} \tag{22}$$

2.2.3 Delayed term interpolated by fourth order interpolation polynomial

When the delayed term $x(ih + h - \xi - T)$ is interpolated by fourth order interpolation polynomial, the nodal values $x(ih + 4h - T)$, $x(ih + 3h - T)$, $x(ih + 2h - T)$, $x(ih + h - T)$, and $x(ih - T)$ denoted as x_{i-n+4} , x_{i-n+3} , x_{i-n+2} , x_{i-n+1} , and x_{i-n} are employed for interpolation. The delayed term $x(ih + h - \xi - T)$ can be expressed as

$$x(ih + h - \xi - T) = \left(\frac{-\xi}{12h} - \frac{\xi^2}{24h^2} + \frac{\xi^3}{12h^3} + \frac{\xi^4}{24h^4} \right) x_{i+4-n} + \left(\frac{\xi}{2h} + \frac{\xi^2}{6h^2} - \frac{\xi^3}{2h^3} - \frac{\xi^4}{6h^4} \right) x_{i+3-n} + \left(\frac{-3\xi}{2h} + \frac{\xi^2}{4h^2} + \frac{\xi^3}{h^3} + \frac{\xi^4}{4h^4} \right) x_{i+2-n} + \left(1 + \frac{5\xi}{6h} - \frac{5\xi^2}{6h^2} - \frac{5\xi^3}{6h^3} - \frac{\xi^4}{6h^4} \right) x_{i+1-n} + \left(\frac{\xi}{4h} + \frac{11\xi^2}{24h^2} + \frac{\xi^3}{4h^3} + \frac{\xi^4}{24h^4} \right) x_{i-n} \tag{23}$$

Combining Eqs. (4) and (23), the following result can be obtained

$$\int_0^h e^{A\xi} \mathbf{B}(ih + h - \xi) \mathbf{x}(ih + h - \xi - T) d\xi = \begin{pmatrix} (\mathbf{H}_{41}\mathbf{B}_{i+1} + \mathbf{H}_{42}\mathbf{B}_i)\mathbf{x}_{i+4-n} + (\mathbf{H}_{43}\mathbf{B}_{i+1} + \mathbf{H}_{44}\mathbf{B}_i)\mathbf{x}_{i+3-n} + (\mathbf{H}_{45}\mathbf{B}_{i+1} + \mathbf{H}_{46}\mathbf{B}_i)\mathbf{x}_{i+2-n} + (\mathbf{H}_{47}\mathbf{B}_{i+1} + \mathbf{H}_{48}\mathbf{B}_i)\mathbf{x}_{i+1-n} + (\mathbf{H}_{49}\mathbf{B}_{i+1} + \mathbf{H}_{410}\mathbf{B}_i)\mathbf{x}_{i-n} \end{pmatrix} \tag{24}$$

where

$$\begin{aligned} \mathbf{H}_{41} &= \frac{-F_2}{12h} + \frac{F_3}{24h^2} + \frac{F_4}{8h^3} - \frac{F_5}{24h^4} - \frac{F_6}{24h^5}, & \mathbf{H}_{42} &= \frac{-F_3}{12h^2} - \frac{F_4}{24h^3} + \frac{F_5}{12h^4} + \frac{F_6}{24h^5} \\ \mathbf{H}_{43} &= \frac{2h}{3F_2} - \frac{3h^2}{7F_3} + \frac{3h^3}{3F_4} + \frac{3h^4}{3F_5} - \frac{F_6}{F_6}, & \mathbf{H}_{44} &= \frac{F_3}{2h^2} + \frac{6h^3}{3F_3} - \frac{2h^4}{F_4} - \frac{6h^5}{F_5} \\ \mathbf{H}_{45} &= -\frac{2h}{3F_2} + \frac{4h^2}{5F_3} + \frac{4h^3}{2F_4} - \frac{4h^4}{5F_5} + \frac{4h^5}{F_6}, & \mathbf{H}_{46} &= -\frac{F_3}{2h^2} + \frac{F_4}{4h^3} + \frac{F_5}{h^4} + \frac{F_6}{4h^5} \\ \mathbf{H}_{47} &= F_1 - \frac{F_2}{6h} - \frac{5F_3}{3h^2} + \frac{2F_4}{3h^3} - \frac{3h^4}{5F_5} + \frac{6h^5}{F_6}, & \mathbf{H}_{48} &= \frac{F_2}{h} + \frac{5F_3}{6h^2} - \frac{5F_4}{6h^3} - \frac{5F_5}{6h^4} - \frac{F_6}{6h^5} \\ \mathbf{H}_{49} &= \frac{F_2}{4h} + \frac{5F_3}{24h^2} - \frac{5F_4}{24h^3} - \frac{5F_5}{24h^4} - \frac{F_6}{24h^5}, & \mathbf{H}_{410} &= \frac{F_3}{4h^2} + \frac{11F_4}{24h^3} + \frac{F_5}{4h^4} + \frac{F_6}{24h^5} \end{aligned} \tag{25}$$

$$\mathbf{x}_{i+1} = (\mathbf{I} - \mathbf{G}_{25}\mathbf{B}_{i+1} - \mathbf{G}_{26}\mathbf{B}_i) \begin{bmatrix} (\mathbf{G}_{23}\mathbf{B}_{i+1} + \mathbf{G}_{24}\mathbf{B}_i + \mathbf{F}_0)\mathbf{x}_i + (\mathbf{G}_{21}\mathbf{B}_{i+1} + \mathbf{G}_{22}\mathbf{B}_i)\mathbf{x}_{i-1} \\ (\mathbf{H}_{21}\mathbf{B}_{i+1} + \mathbf{H}_{22}\mathbf{B}_i)\mathbf{x}_{i+2-n} - (\mathbf{H}_{23}\mathbf{B}_{i+1} + \mathbf{H}_{24}\mathbf{B}_i)\mathbf{x}_{i+1-n} \\ (\mathbf{H}_{25}\mathbf{B}_{i+1} + \mathbf{H}_{26}\mathbf{B}_i)\mathbf{x}_{i-n} \end{bmatrix} \tag{26}$$

According to Eq. (26), the following discrete mapping can be acquired

$$\mathbf{y}_{i+1} = \mathbf{D}_i \mathbf{y}_i \tag{27}$$

where \mathbf{y}_i can be written as

2.3 The stability analysis methods

2.3.1 The 2nd-2nd HFDm

As is stated above, in the 2nd-2nd HFDm, the state term and delayed term are both interpolated by second order interpolation polynomials.

Combining Eqs. (3), (6), and (18), a map relation can be obtained using 2nd-2nd HFDm as follow

$$\mathbf{y}_i = [\mathbf{x}_i \ \mathbf{x}_{i-1} \ \mathbf{x}_{i-2} \ \dots \ \mathbf{x}_{i-n+1} \ \mathbf{x}_{i-n}]^T \tag{28}$$

The matrix \mathbf{D}_i ($i = 0, 1, \dots, n - 1$) can be expressed as

$$\mathbf{D}_i = \begin{bmatrix} \mathbf{P}_i(\mathbf{G}_{23}\mathbf{B}_{i+1} + \mathbf{G}_{24}\mathbf{B}_i + \mathbf{F}_0) & \mathbf{P}_i(\mathbf{G}_{21}\mathbf{B}_{i+1} + \mathbf{G}_{22}\mathbf{B}_i) & \mathbf{0} & \dots & -\mathbf{P}_i(\mathbf{H}_{21}\mathbf{B}_{i+1} + \mathbf{H}_{22}\mathbf{B}_i) & -\mathbf{P}_i(\mathbf{H}_{23}\mathbf{B}_{i+1} + \mathbf{H}_{24}\mathbf{B}_i) & -\mathbf{P}_i(\mathbf{H}_{25}\mathbf{B}_{i+1} + \mathbf{H}_{26}\mathbf{B}_i) \\ \mathbf{I} & \mathbf{0} & \mathbf{0} & \dots & \mathbf{0} & \mathbf{0} & \mathbf{0} \\ \mathbf{0} & \mathbf{I} & \mathbf{0} & \dots & \mathbf{0} & \mathbf{0} & \mathbf{0} \\ \mathbf{0} & \mathbf{0} & \mathbf{I} & \dots & \mathbf{0} & \mathbf{0} & \mathbf{0} \\ \vdots & \vdots & \vdots & \ddots & \vdots & \vdots & \vdots \\ \mathbf{0} & \mathbf{0} & \mathbf{0} & \dots & \mathbf{I} & \mathbf{0} & \mathbf{0} \\ \mathbf{0} & \mathbf{0} & \mathbf{0} & \dots & \mathbf{0} & \mathbf{I} & \mathbf{0} \end{bmatrix} \tag{29}$$

where \mathbf{P}_i can be expressed by

$$\mathbf{P}_i = (\mathbf{I} - \mathbf{G}_{25}\mathbf{B}_{i+1} - \mathbf{G}_{26}\mathbf{B}_i) \tag{30}$$

The state transition matrix Ψ for the dynamic system over one period T is written as

$$\Psi = \mathbf{D}_{n-1} \mathbf{D}_{n-2} \dots \mathbf{D}_0 \tag{31}$$

Then, the stability of the milling system can be determined according to Floquet theory: if the modulus of the maximal

eigenvalue of the transition matrix Ψ is less than one, the system is stable; if the modulus of the maximal eigenvalue of the transition matrix Ψ is equal to one, the system is critical stable; otherwise, unstable.

2.3.2 The 2nd-3rd HFDm

Combining Eqs. (3), (6), and (21), the following map can be obtained using 2nd-3rd HFDm:

$$\mathbf{x}_{i+1} = (\mathbf{I} - \mathbf{G}_{25}\mathbf{B}_{i+1} - \mathbf{G}_{26}\mathbf{B}_i) \begin{bmatrix} (\mathbf{G}_{23}\mathbf{B}_{i+1} + \mathbf{G}_{24}\mathbf{B}_i + \mathbf{F}_0)\mathbf{x}_i + (\mathbf{G}_{21}\mathbf{B}_{i+1} + \mathbf{G}_{22}\mathbf{B}_i)\mathbf{x}_{i-1}^- \\ (\mathbf{H}_{31}\mathbf{B}_{i+1} + \mathbf{H}_{32}\mathbf{B}_i)\mathbf{x}_{i+3-n} - (\mathbf{H}_{33}\mathbf{B}_{i+1} + \mathbf{H}_{34}\mathbf{B}_i)\mathbf{x}_{i+2-n}^- \\ (\mathbf{H}_{35}\mathbf{B}_{i+1} + \mathbf{H}_{36}\mathbf{B}_i)\mathbf{x}_{i+1-n} - (\mathbf{H}_{37}\mathbf{B}_{i+1} + \mathbf{H}_{38}\mathbf{B}_i)\mathbf{x}_{i-n}^- \end{bmatrix} \tag{32}$$

Similar to the 2nd-2nd HFDM, a discrete mapping can be obtained according to Eq. (32). Then, the stability of the milling system also can be predicted using 2nd-3rd HFDM based on Floquet theory.

2.3.3 The 2nd-4th HFDM

Substituting Eqs. (6) and (24) into Eq. (3) yields

$$\mathbf{x}_{i+1} = (\mathbf{I} - \mathbf{G}_{25}\mathbf{B}_{i+1} - \mathbf{G}_{26}\mathbf{B}_i) \begin{bmatrix} (\mathbf{G}_{23}\mathbf{B}_{i+1} + \mathbf{G}_{24}\mathbf{B}_i + \mathbf{F}_0)\mathbf{x}_i + (\mathbf{G}_{21}\mathbf{B}_{i+1} + \mathbf{G}_{22}\mathbf{B}_i)\mathbf{x}_{i-1}^- \\ (\mathbf{H}_{41}\mathbf{B}_{i+1} + \mathbf{H}_{42}\mathbf{B}_i)\mathbf{x}_{i+4-n} - (\mathbf{H}_{43}\mathbf{B}_{i+1} + \mathbf{H}_{44}\mathbf{B}_i)\mathbf{x}_{i+3-n}^- \\ (\mathbf{H}_{45}\mathbf{B}_{i+1} + \mathbf{H}_{46}\mathbf{B}_i)\mathbf{x}_{i+2-n} - (\mathbf{H}_{47}\mathbf{B}_{i+1} + \mathbf{H}_{48}\mathbf{B}_i)\mathbf{x}_{i+1-n}^- \\ (\mathbf{H}_{49}\mathbf{B}_{i+1} + \mathbf{H}_{410}\mathbf{B}_i)\mathbf{x}_{i-n}^- \end{bmatrix} \tag{33}$$

According to Eq. (33), the discrete mapping calculated by 2nd-4th HFDM can be obtained and expressed in the form of Eq. (27). Similarly, the stability of the milling system can also be determined using 2nd-4th HFDM based on Floquet theory.

The discrete mappings obtained by 3rd-2nd HFDM, 3rd-3rd HFDM, 3rd-4th HFDM, 4th-2nd HFDM, 4th-3rd HFDM, and 4th-4th HFDM are given in Appendix.

3 Model verification

3.1 Computational accuracy analysis

The rate of convergence can be used to estimate the computational accuracy of discretization methods, which reflects how fast the approximated modulus of the maximal critical eigenvalues of the milling system $|\mu(n)|$ converge to an exact value $|\mu_0|$, where $|\mu(n)|$ is a function of the parameter n . That is, the rate of convergence can also be used to estimate the local discretization errors between $|\mu(n)|$ and the $|\mu_0|$. In order to demonstrate the rate of convergence of different HFDMs, a 1-DOF milling dynamic system is taken for verification.

For the 1-DOF milling dynamic system, the matrixes \mathbf{A} , $\mathbf{B}(t)$, and $\mathbf{x}(t)$ can be given as

$$\mathbf{A} = \begin{bmatrix} 0 & 1 \\ -\omega_n^2 & -2\zeta\omega_n \end{bmatrix}, \mathbf{B}(t) = \begin{bmatrix} 0 & 0 \\ -\frac{a_p h(t)}{m_t} & 0 \end{bmatrix}, \tag{34}$$

$$\mathbf{x}(t) = \begin{bmatrix} x(t) \\ \dot{x}(t) \end{bmatrix}$$

where ζ is the damping ratio, ω_n is the angular natural frequency, a_p is the axial depth of cut, m_t is the modal mass, $x(t)$ is the

displacement in the X direction, and the instantaneous chip thickness $h(t)$ can be written as

$$h(t) = \sum_{j=1}^N g[\varphi_j(t)] \sin(\varphi_j(t)) [K_t \cos(\varphi_j(t)) + K_n \sin(\varphi_j(t))] \tag{35}$$

where K_t and K_n are the tangential and the normal cutting force coefficients, respectively, and N is the number of cutter teeth. The angular position of the j th tooth $\varphi_j(t)$ is determined as

$$\varphi_j(t) = (2\pi\Omega/60)t + (j-1)2\pi/N \tag{36}$$

where Ω denotes the spindle speed in rpm. The function $g[\varphi_j(t)]$ is a unit step function which determines whether the tooth is in or out of cut.

It is pointed out in literature [33] that the DFDMs have an advantage over the existing FDMs in terms of the convergence rate. In addition, the rate of convergence of the 4th DFDM is also proved to be higher than those of the 1st DFDM, 2nd DFDM, and 3rd DFDM. Therefore, the 4th DFDM as well as the existing 2nd UFDM and 3rd UFDM are taken as benchmark for comparing with different HFDMs. To demonstrate the rates of convergence of different HFDMs, the radial immersion ratio is set as $a_e/D = 1$, and the other main parameters derived from the literature [12] are adopted in this work, as shown in Table 1. The program is conducted using MATLAB 2017a software on a computer with Intel (R) Core (TM) i7-7700U and 16 GB memory.

To illustrate the rates of convergence of different HFDMs, the convergence of the function $|\mu(n)|$ to an exact value is studied. The process parameter points ($\Omega = 6700$ rpm, $a_p = 2.6667$ mm) and ($\Omega = 8612.5$ rpm, $a_p = 2.5$ mm) which are adopted in literature [29] are also employed to analyze the rates of convergence for different HFDMs, as shown in Fig. 1.

Table 1 The parameters of milling system

Parameters	Value
Teeth number N	2
The natural frequency ω_n (Hz)	922
Damping ratio	0.011
Modal mass m_t (kg)	0.03993
The tangential cutting force coefficient K_t (N/m ²)	6×10^8
The normal cutting force coefficient K_n (N/m ²)	2×10^8
Milling type	Down milling

In the existing 2nd UFD, the state transition matrix is obtained based on the periodicity of the dynamic response. In the 2nd-2nd HFDM in this work, the state transition matrix is obtained by coupling a sequence of discrete map. However, it should be noted that the rate of convergence of the 2nd-2nd HFDM is identical with that of the existing 2nd UFD, since the state term and delayed term of these two methods are approximated by the same interpolation polynomials. Similarly, the rate of convergence of the 3rd-3rd HFDM is also identical with that of the existing 3rd UFD.

It can be seen from Fig. 1 that the 3rd-2nd HFDM converges faster than the other methods. As shown in Fig. 1 a and b, the 3rd-2nd HFDM achieves the convergence when n is equal to 35, while the other methods achieve the convergence when n is greater than 35.

In mathematical theory, higher order interpolation for the state term and delayed term can lead to more accurate results. The state term and delayed term of the 4th-4th HFDM are both interpolated by fourth order interpolation polynomials; however, the 4th-4th HFDM does not converge the fastest among the HFDMs. Additionally, compared with the 3rd-2nd

HFDM, the much higher order interpolation is used to approximate the state term of the 4th-2nd HFDM. However, it can be seen from Fig. 1 that the 3rd-2nd HFDM converges a little faster than the 4th-2nd HFDM. Therefore, higher order interpolation for the state term and delayed term does not necessarily lead to more accurate results in the stability analysis using HFDMs.

Since the stability prediction method is sensitive to the process parameters, more process parameter points are employed for the analysis of rate of convergence. In the following analysis, the local discretization errors between the function $|\mu(n)|$ and the exact value $|\mu_0|$ are used to evaluate the rate of convergence, and $|\mu_0|$ is determined by the 1stSDM with $n = 600$. The radial immersion ratio a_e/D is also set as 1, the spindle speeds Ω is set as 5000, 7000, and 9000 rpm, and the axial depth of cut a_p is chosen as 0.5, 1.0, 2.0, and 3.0 mm. The rates of convergence of different HFDMs with different values of discretization parameter n are illustrated in Table 2.

It can be seen from Table 2 that the 4th-2nd HFDM converges faster than the other methods when the process parameter point is ($\Omega = 5000$ rpm, $a_p = 2.0$ mm), while it converges slower than the other methods when the process parameter point is ($\Omega = 9000$ rpm, $a_p = 3.0$ mm). Besides, as shown in Table 2, under the condition of the same axial depth of cut ($a_p = 3.0$ mm), the local discretization errors calculated by the 4th DFDM are smaller than those calculated by most of the HFDMs when the spindle speed is $\Omega = 5000$ rpm but greater than those calculated by different HFDMs when the spindle speed is $\Omega = 7000$ rpm. Therefore, it is difficult to evaluate the accuracy of different methods through the convergence rate analysis of limited process parameter points.

With the aim of further estimating the accuracy of different HFDMs, the mean difference M and variance V which are used in literature [24] are employed in this work, and expressed by

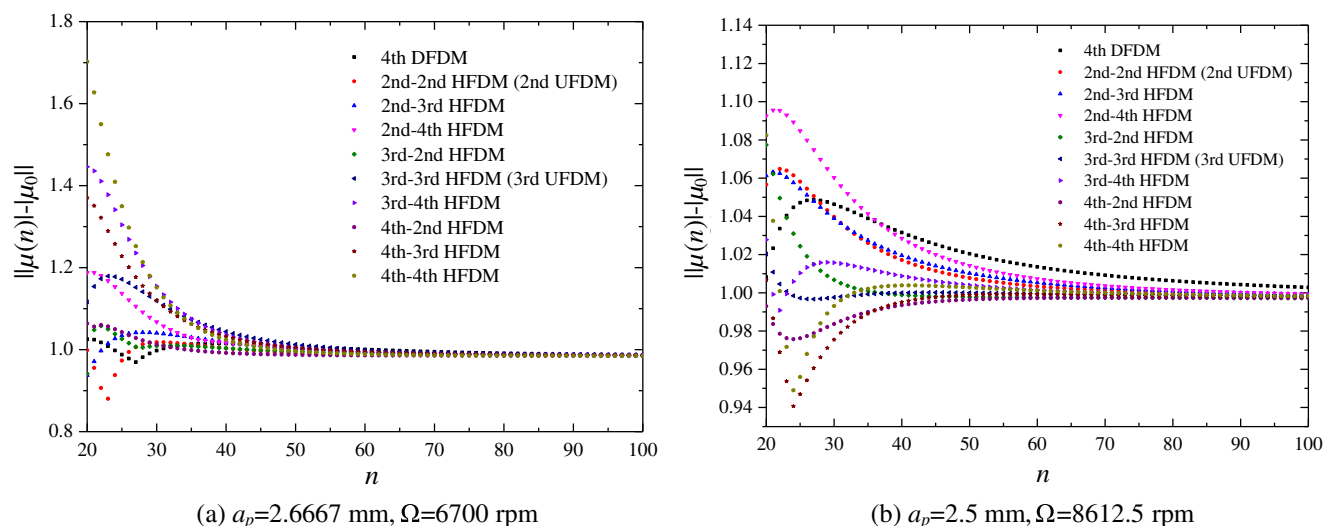
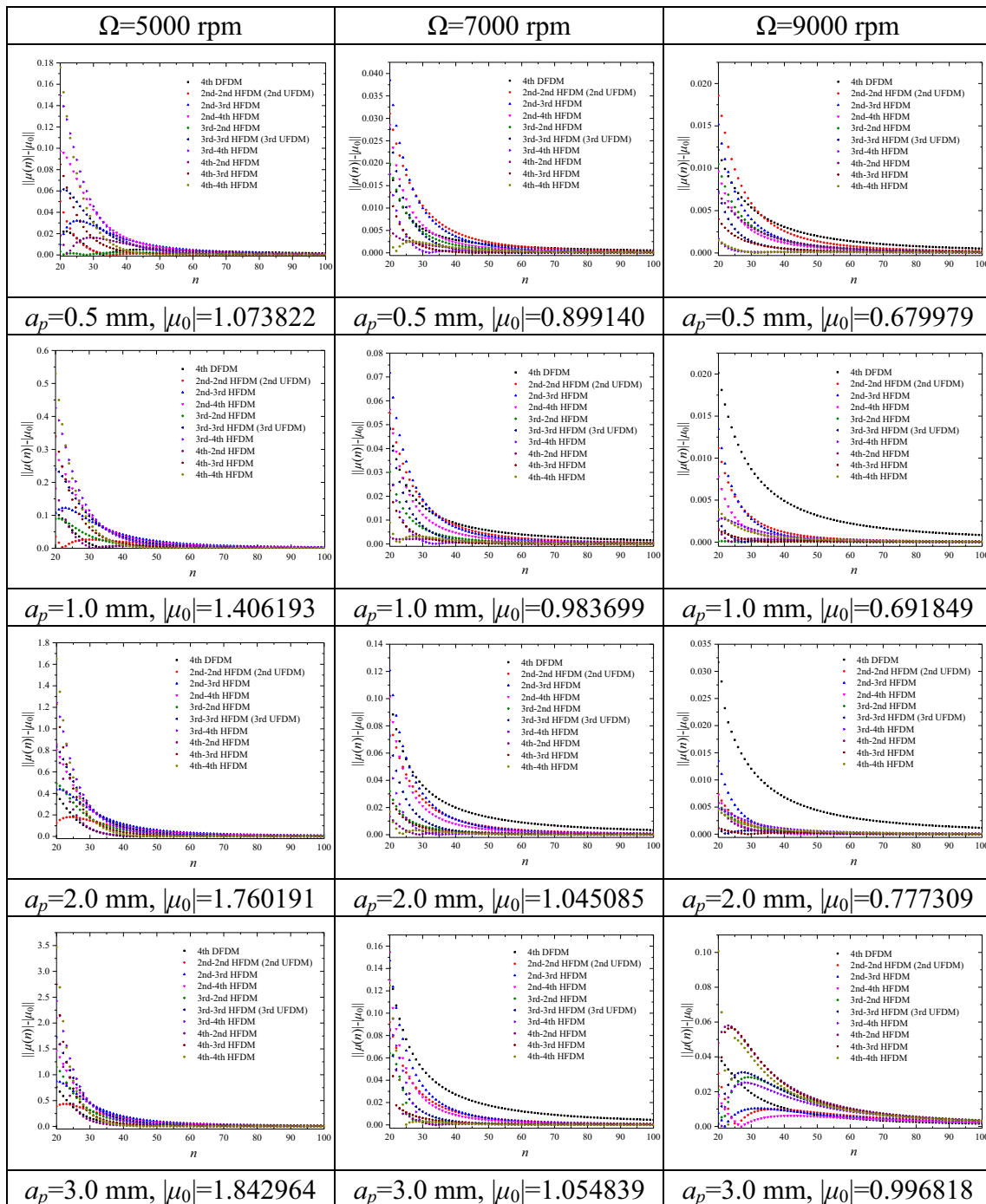
**Fig. 1** The convergence of $|\mu(n)|$ for different HFDMs. **a** $a_p = 2.6667$ mm, $\Omega = 6700$ rpm; **b** $a_p = 2.5$ mm, $\Omega = 8612.5$ rpm

Table 2 The rates of convergence of the HFDMs with different values of discretization parameter n



$$M = \frac{1}{r} \sum_{i=1}^r |a_{p,i} - a_{p,i0}|, V = \frac{1}{r} \sum_{i=1}^r (a_{p,i} - a_{p,i0})^2 \quad (37)$$

where $a_{p,i}$ and $a_{p,i0}$ are the referenced and predicted critical depths of cut at i th discrete spindle speed, respectively; r is the number of discrete points in range of spindle speed. The referenced depth of cut at i th discrete spindle speed is extracted from the stability lobe diagram with $n = 200$, and the predicted

critical depths of cut are extracted from the stability lobe diagrams with different values of discretization parameter n . The stability lobe diagrams are calculated over 250×250 sized equidistance grid of spindle speed and axial depth of cut. The spindle speed ranges from 5000 to 10,000 rpm, and the axial depth of cut ranges from 0 to 10 mm. The comparisons of the mean difference and variance calculated by different methods with the radial immersion ratio $a_e/D = 1$ are shown in Fig. 2.

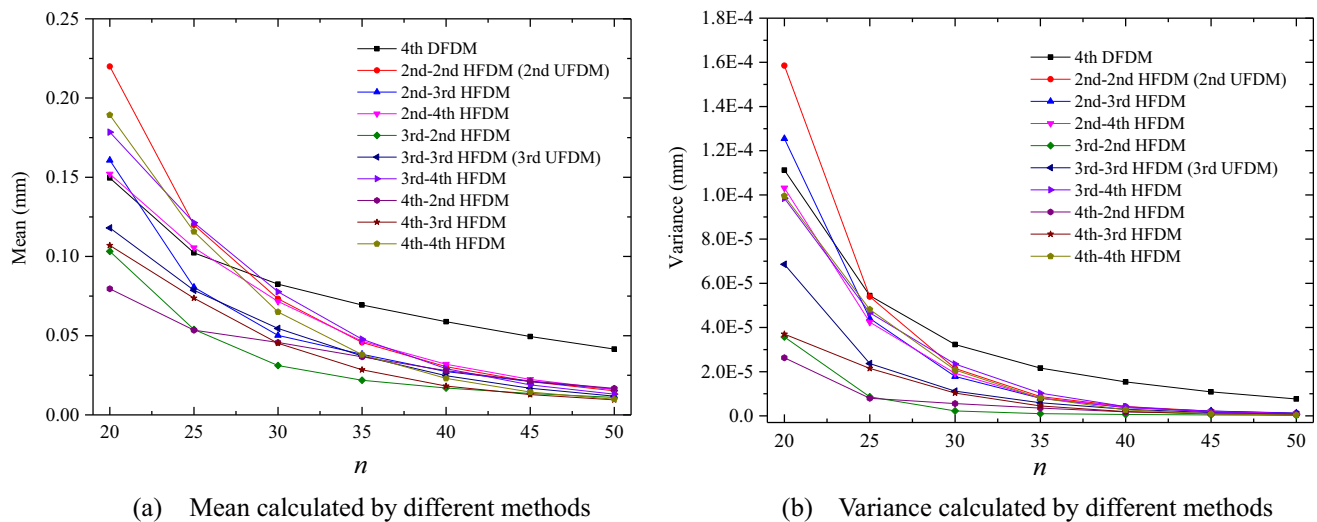


Fig. 2 Comparisons of the **a** mean and **b** variance calculated by different methods with the radial immersion ratio $a_e/D = 1$

It is seen from Fig. 2 that the mean differences and variances between $a_{p,i}$ and $a_{p,i0}$ decrease with the increase of the discretization parameter n . When the parameter n is between 25 and 40, the mean differences obtained by 3rd-2nd HFDM are less than those obtained by the other methods. Meanwhile, the mean differences obtained by 3rd-2nd HFDM, 4th-3rd HFDM, and 4th-4th HFDM are almost equal when n is greater than 40, and the corresponding mean differences obtained by these three methods are less than those obtained by the other methods. Therefore, the 3rd-2nd HFDM is, on the whole, more accurate than the other methods. Besides, as shown in Fig. 2b, the variances calculated by 3rd-2nd HFDM are less than those calculated by the other methods, which indicates that the fluctuation of the mean differences obtained by 3rd-2nd HFDM is smaller than those calculated by the other methods. The stability lobe diagrams generated by using different HFDMs with different values of the discretization parameter n are also presented, as shown in Table 3.

According to Table 3, it can be seen that the stability lobe diagrams obtained by 3rd-2nd HFDM are closer to the referenced one when the discretization parameter n is chosen as 30 and 40. When the discretization parameter n is equal to 50, the stability lobe diagrams obtained by 3rd-2nd HFDM, 4th-3rd HFDM, and 4th-4th HFDM are all highly consistent with the referenced one. The results illustrated in Table 3 are consistent with those obtained by calculating the mean differences and variances between the referenced and predicted critical depths of cut.

3.2 Computational efficiency

3.2.1 Stability lobe diagrams for 1-DOF milling system

To demonstrate the computational efficiency of different HFDMs, a time-consuming study is conducted. The stability

lobe diagrams are calculated over 200×100 sized equidistance grid of spindle speed and axial depth of cut. The spindle speed ranges from 5000 to 10,000 rpm, and the axial depth of cut ranges from 0 to 10 mm. The radial immersion ratio a_e/D is set as 0.1 and 0.6, and the corresponding parameter n is chosen as 30 and 40, respectively. The stability lobe diagrams calculated by 2nd UFDM with $n = 100$ are taken as the referenced lobe diagrams denoted with red line. The parameters employed to obtain the stability lobe diagrams are the same with the parameters listed in Table 1. The stability lobe diagrams denoted with black line are predicted by different methods. The stability lobe diagrams as well as the computational time are listed in Table 4.

The computational time of different HFDMs is related to the number of matrixes (“G” matrixes and “H” matrixes). As shown in Table 4, the computational time spent by 4th DFDM, 2nd-3rd HFDM, and 3rd-2nd HFDM for obtaining stability lobe diagrams are very close since the number of matrixes of these three methods is the same. The 4th-4th HFDM spends more computation time than the other methods since the number of matrixes of 4th-4th HFDM is most. The 2nd UFDM consumes the least time to obtain the stability lobe diagrams due to the small number of matrixes. The time increment between the 3rd-2nd HFDM and 2nd UFDM is small because the increment of matrix number between these two methods is also small. Therefore, the 3rd-2nd is also an efficient method.

3.3 Stability lobe diagrams of 2-DOF milling system

To further verify the effectiveness of different HFDMs, the 2-DOF milling system is also considered. The stability lobe diagrams are calculated over 200×100 sized equidistance grid of spindle speed and axial depth of cut. The spindle speed ranges from 5000 to 25,000 rpm, and the axial depth of cut

Table 3 The stability lobe diagrams generated by using different HFDMs with different values of the discretization parameter n

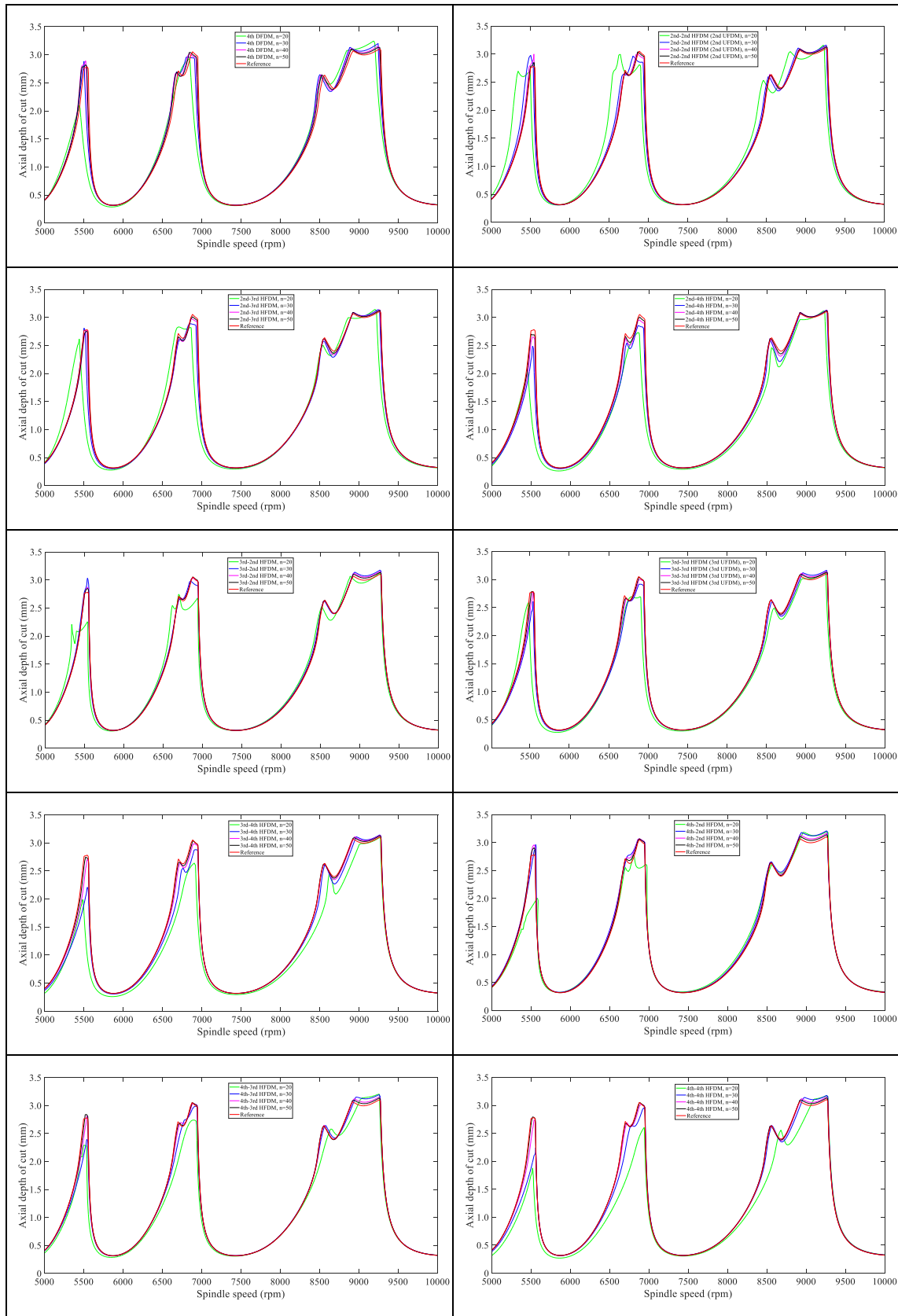
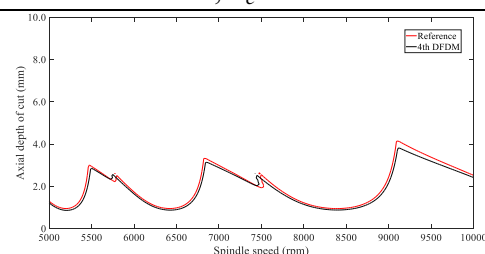
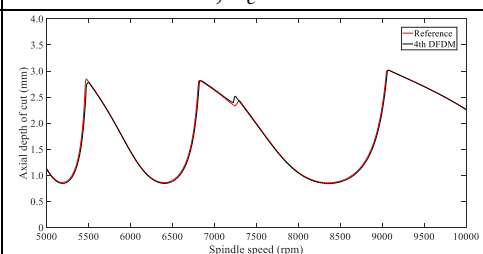
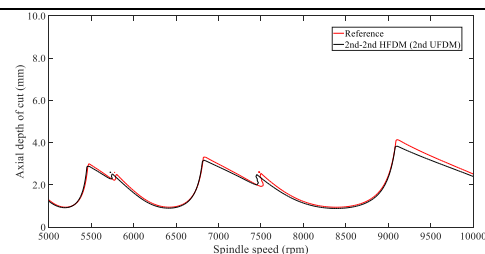
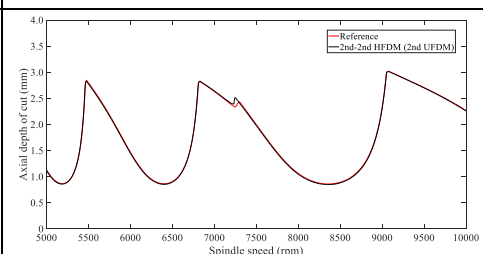
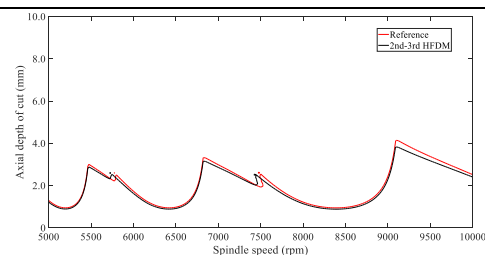
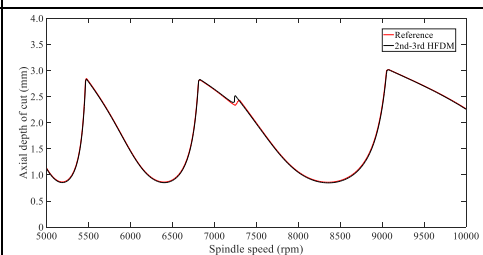
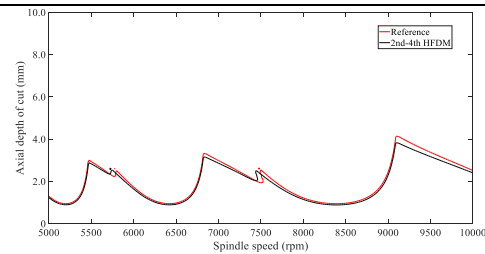
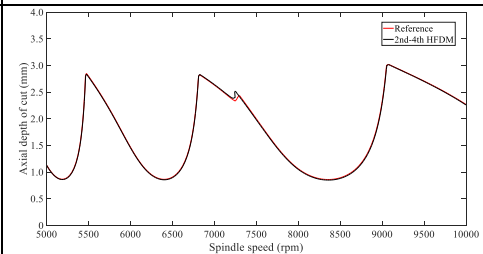
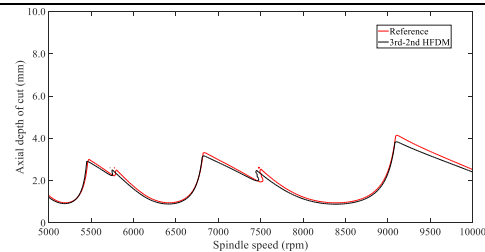
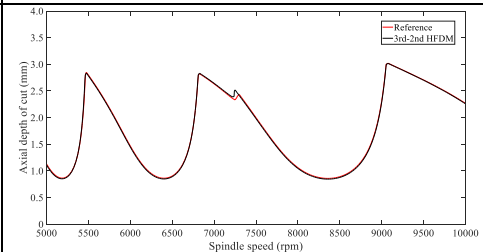
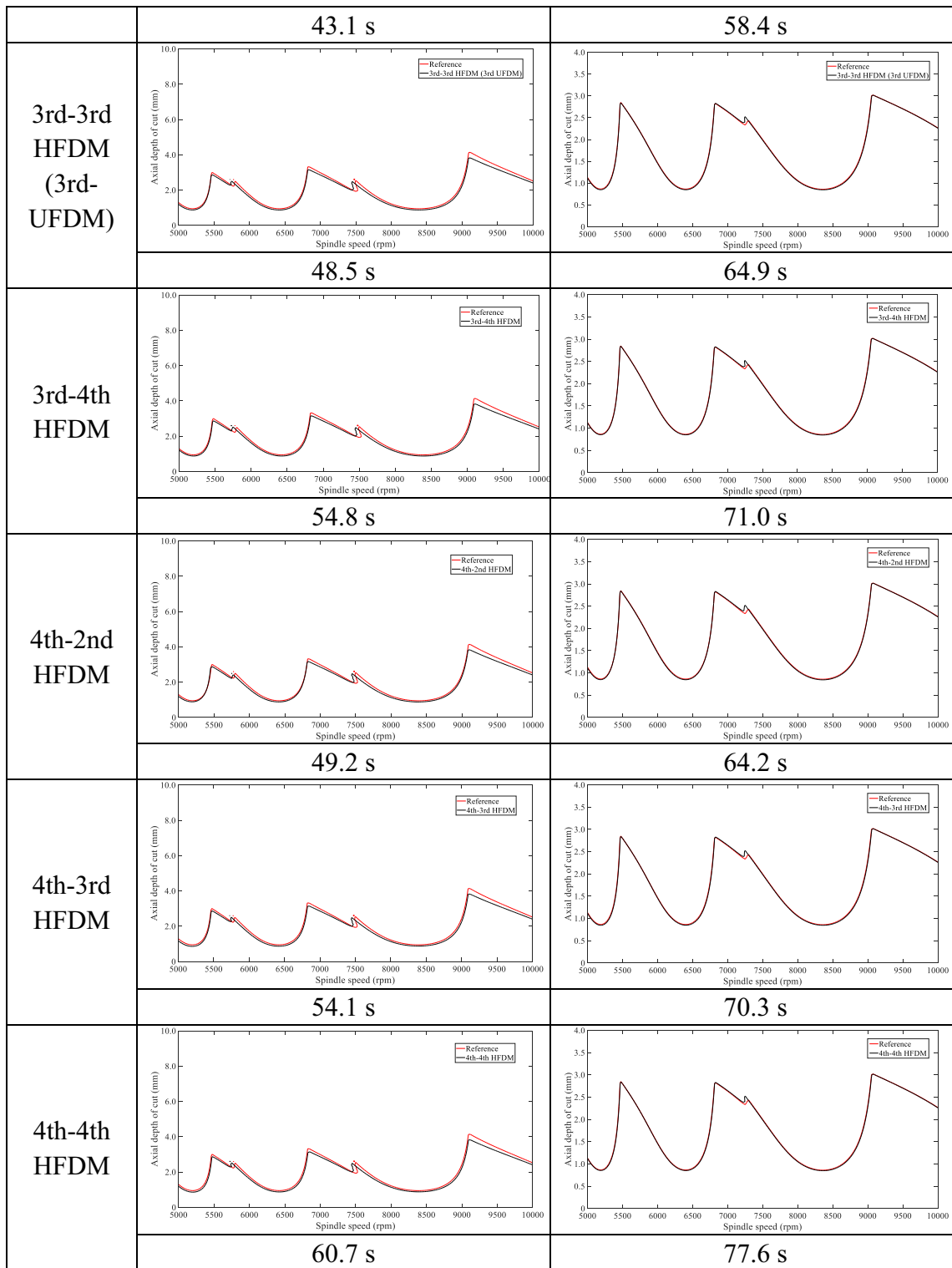


Table 4 The stability lobe diagrams obtained by different methods for 1-DOF milling system

Methods	$n=30, a_e/D=0.1$	$n=40, a_e/D=0.6$
4th-DFDM	 <p>43.2 s</p>	 <p>59.2 s</p>
2nd-2nd HFDM (2nd-UFDM)	 <p>39.1 s</p>	 <p>53.6 s</p>
2nd-3rd HFDM	 <p>44.4 s</p>	 <p>58.7 s</p>
2nd-4th HFDM	 <p>48.9 s</p>	 <p>65.5 s</p>
3rd-2nd HFDM		

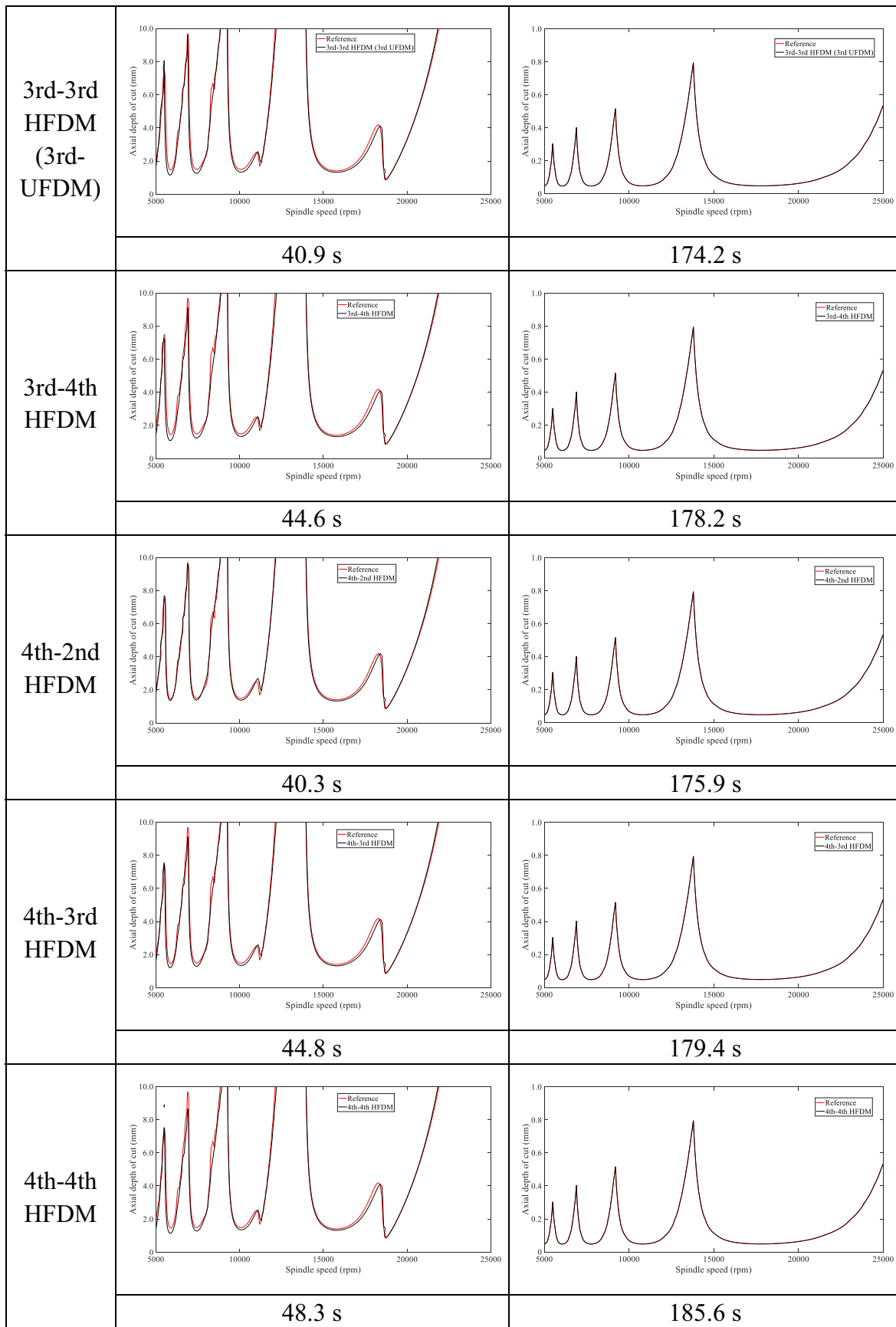


ranges from 0 to 10 mm. The radial immersion ration a_p/D is set as 0.05 and 1, and the corresponding parameter n is chosen as 20 and 40, respectively. The referenced stability lobe diagrams are calculated by 2nd UFDM with $n = 100$ and denoted with red line. The adopted parameters are the same with those

listed in Table 1, and the modal parameters are assumed to be equal in X and Y directions. The stability lobe diagrams predicted by different methods are denoted with black line. The stability lobe diagrams as well as the computational time are listed in Table 5.

Table 5 The stability lobe diagrams obtained by different methods for 2-DOF milling system

Method s	$n=20, a_e/D=0.05$	$n=40, a_e/D=1$
4th-DFDM		
	37.6 s	162.6 s
2nd-2nd HFDM (2nd-UFDM)		
	33.2 s	153.3 s
2nd-3rd HFDM		
	37.1 s	166.7 s
2nd-4th HFDM		
	41.0 s	172.0 s
3rd-2nd HFDM		
	36.9 s	160.6 s



It can be seen from Table 5 that the HFDMs are available for predicting the stability lobe diagrams under both large immersion condition ($a_e/D = 1$) and low immersion condition ($a_e/D = 0.05$). As shown in Table 5, it is found that the stability lobe diagram obtained by 3rd-2nd HFDM is closer to the referenced one when the radial immersion ratio a_e/D is set as 0.05. Just like the result observed in 1-DOF milling system, the computational time of different HFDMs for 2-DOF is also affected by the number of matrixes. For instance, when $n = 40$ and $a_e/D = 1$, the 3rd-2nd HFDM, 3rd-3rd HFDM, and 3rd-4th HFDM take 36.9, 40.9, and 44.6 s to obtain the stability lobe diagrams, respectively. The 3rd-2nd HFDM consumes less time than the 3rd-3rd HFDM and 3rd-4th HFDM to generate the stability lobe diagrams since less matrixes need to be calculated. When $n = 40$ and $a_e/D = 1$, the stability lobe diagrams obtained by different HFDMs are high coincidence with the referenced ones.

The 4th DFDM is proved to be an efficient method for milling stability analysis. It is indicated from Table 5 that the computational time of 3rd-2nd HFDM is almost the same with that of the 4th DFDM. Therefore, the 3rd-2nd HFDM can be used to predict the milling stability efficiently.

4 Conclusion

This paper focuses on comparing different HFDMs from the aspects of accuracy and efficiency. The following conclusions can be drawn:

- (1) Higher order interpolation for the state term and delayed term does not necessarily lead to more accurate results in the stability analysis using HFDMs.
- (2) It is difficult to evaluate the accuracy of different HFDMs through the convergence rate analysis of limited process parameter points.
- (3) The mean differences and variances between the referenced and predicted critical depths of cut are employed for accuracy analysis. The 3rd-2nd HFDM is, on the whole, proved to be more accurate than the other methods.
- (4) The HFDMs are available for predicting the stability lobe diagrams under both large immersion condition and low immersion condition.
- (5) The computational time of different HFDMs is related to the number of matrixes. The 3rd-2nd HFDM is proved to be an efficient method by comparing with the other methods.

Funding information This work was partially supported by the National Natural Science Foundation of China (Grant No. 51805404), and Open Research Fund Program of Shaanxi Key Laboratory of Non-Traditional Machining (Grant No. 2017SXTZKFJG08) and the Natural Science Basic Research Plan in Shaanxi Province of China (Grant No. 2019JQ-147 and No. 2018JQ5127), and the China Postdoctoral Science Foundation (Grant No. 2019M653570), and the Projects of Science and Technology Department in Shaanxi Province (No.2014JM2-5072, No. 2014SZS20-Z02, and No. 2014SZS20-P06), and the Key Laboratory Research Program Funded by Education Department of Shaanxi Province (No. 18JS045).

Appendix

Combining Eqs. (3), (10), and (18), a discrete mapping can be obtained using 3rd-2nd HFDM as follow

$$\mathbf{x}_{i+1} = (\mathbf{I} - \mathbf{G}_{37}\mathbf{B}_{i+1} - \mathbf{G}_{38}\mathbf{B}_i) \begin{bmatrix} (\mathbf{G}_{35}\mathbf{B}_{i+1} + \mathbf{G}_{36}\mathbf{B}_i + \mathbf{F}_0)\mathbf{x}_i + (\mathbf{G}_{33}\mathbf{B}_{i+1} + \mathbf{G}_{34}\mathbf{B}_i)\mathbf{x}_{i-1} + \\ (\mathbf{G}_{31}\mathbf{B}_{i+1} + \mathbf{G}_{32}\mathbf{B}_i)\mathbf{x}_{i-2} - (\mathbf{H}_{21}\mathbf{B}_{i+1} + \mathbf{H}_{22}\mathbf{B}_i)\mathbf{x}_{i+2-n} \\ - (\mathbf{H}_{23}\mathbf{B}_{i+1} + \mathbf{H}_{24}\mathbf{B}_i)\mathbf{x}_{i+1-n} - (\mathbf{H}_{25}\mathbf{B}_{i+1} + \mathbf{H}_{26}\mathbf{B}_i)\mathbf{x}_{i-n} \end{bmatrix} \quad (38)$$

Combining Eqs. (3), (10), and (21), a discrete mapping can be obtained using 3rd-3rd HFDM as follow

$$\mathbf{x}_{i+1} = (\mathbf{I} - \mathbf{G}_{37}\mathbf{B}_{i+1} - \mathbf{G}_{38}\mathbf{B}_i) \begin{bmatrix} (\mathbf{G}_{35}\mathbf{B}_{i+1} + \mathbf{G}_{36}\mathbf{B}_i + \mathbf{F}_0)\mathbf{x}_i + (\mathbf{G}_{33}\mathbf{B}_{i+1} + \mathbf{G}_{34}\mathbf{B}_i)\mathbf{x}_{i-1} + \\ (\mathbf{G}_{31}\mathbf{B}_{i+1} + \mathbf{G}_{32}\mathbf{B}_i)\mathbf{x}_{i-2} - (\mathbf{H}_{31}\mathbf{B}_{i+1} + \mathbf{H}_{32}\mathbf{B}_i)\mathbf{x}_{i+3-n} - \\ (\mathbf{H}_{33}\mathbf{B}_{i+1} + \mathbf{H}_{34}\mathbf{B}_i)\mathbf{x}_{i+2-n} - (\mathbf{H}_{35}\mathbf{B}_{i+1} + \mathbf{H}_{36}\mathbf{B}_i)\mathbf{x}_{i+1-n} - \\ (\mathbf{H}_{37}\mathbf{B}_{i+1} + \mathbf{H}_{38}\mathbf{B}_i)\mathbf{x}_{i-n} \end{bmatrix} \quad (39)$$

Combining Eqs. (3), (10), and (24), a discrete mapping can be obtained using 3rd-4th HFDM as follow

$$\mathbf{x}_{i+1} = (\mathbf{I} - \mathbf{G}_{37}\mathbf{B}_{i+1} - \mathbf{G}_{38}\mathbf{B}_i) \begin{bmatrix} (\mathbf{G}_{35}\mathbf{B}_{i+1} + \mathbf{G}_{36}\mathbf{B}_i + \mathbf{F}_0)\mathbf{x}_i + (\mathbf{G}_{33}\mathbf{B}_{i+1} + \mathbf{G}_{34}\mathbf{B}_i)\mathbf{x}_{i-1} + \\ (\mathbf{G}_{31}\mathbf{B}_{i+1} + \mathbf{G}_{32}\mathbf{B}_i)\mathbf{x}_{i-2} - (\mathbf{H}_{41}\mathbf{B}_{i+1} + \mathbf{H}_{42}\mathbf{B}_i)\mathbf{x}_{i+4-n} - \\ (\mathbf{H}_{43}\mathbf{B}_{i+1} + \mathbf{H}_{44}\mathbf{B}_i)\mathbf{x}_{i+3-n} - (\mathbf{H}_{45}\mathbf{B}_{i+1} + \mathbf{H}_{46}\mathbf{B}_i)\mathbf{x}_{i+2-n} - \\ (\mathbf{H}_{47}\mathbf{B}_{i+1} + \mathbf{H}_{48}\mathbf{B}_i)\mathbf{x}_{i+1-n} - (\mathbf{H}_{49}\mathbf{B}_{i+1} + \mathbf{H}_{410}\mathbf{B}_i)\mathbf{x}_{i-n} \end{bmatrix} \quad (40)$$

Combining Eqs. (3), (14), and (18), a discrete mapping can be obtained using 4th-2nd HFDM as follow

$$\mathbf{x}_{i+1} = (\mathbf{I} - \mathbf{G}_{49}\mathbf{B}_{i+1} - \mathbf{G}_{410}\mathbf{B}_i) \begin{bmatrix} (\mathbf{G}_{47}\mathbf{B}_{i+1} + \mathbf{G}_{48}\mathbf{B}_i + \mathbf{F}_0)\mathbf{x}_i + (\mathbf{G}_{45}\mathbf{B}_{i+1} + \mathbf{G}_{46}\mathbf{B}_i)\mathbf{x}_{i-1} + \\ (\mathbf{G}_{43}\mathbf{B}_{i+1} + \mathbf{G}_{44}\mathbf{B}_i)\mathbf{x}_{i-2} + (\mathbf{G}_{41}\mathbf{B}_{i+1} + \mathbf{G}_{42}\mathbf{B}_i)\mathbf{x}_{i-3} - \\ (\mathbf{H}_{21}\mathbf{B}_{i+1} + \mathbf{H}_{22}\mathbf{B}_i)\mathbf{x}_{i+2-n} - (\mathbf{H}_{23}\mathbf{B}_{i+1} + \mathbf{H}_{24}\mathbf{B}_i)\mathbf{x}_{i+1-n} \\ - (\mathbf{H}_{25}\mathbf{B}_{i+1} + \mathbf{H}_{26}\mathbf{B}_i)\mathbf{x}_{i-n} \end{bmatrix} \quad (41)$$

Combining Eqs. (3), (14), and (21), a discrete mapping can be obtained using 4th-3rd HFDM as follow

$$\mathbf{x}_{i+1} = (\mathbf{I} - \mathbf{G}_{49}\mathbf{B}_{i+1} - \mathbf{G}_{410}\mathbf{B}_i) \begin{bmatrix} (\mathbf{G}_{47}\mathbf{B}_{i+1} + \mathbf{G}_{48}\mathbf{B}_i + \mathbf{F}_0)\mathbf{x}_i + (\mathbf{G}_{45}\mathbf{B}_{i+1} + \mathbf{G}_{46}\mathbf{B}_i)\mathbf{x}_{i-1} + \\ (\mathbf{G}_{43}\mathbf{B}_{i+1} + \mathbf{G}_{44}\mathbf{B}_i)\mathbf{x}_{i-2} + (\mathbf{G}_{41}\mathbf{B}_{i+1} + \mathbf{G}_{42}\mathbf{B}_i)\mathbf{x}_{i-3} - \\ (\mathbf{H}_{31}\mathbf{B}_{i+1} + \mathbf{H}_{32}\mathbf{B}_i)\mathbf{x}_{i+3-n} - (\mathbf{H}_{33}\mathbf{B}_{i+1} + \mathbf{H}_{34}\mathbf{B}_i)\mathbf{x}_{i+2-n} - \\ (\mathbf{H}_{35}\mathbf{B}_{i+1} + \mathbf{H}_{36}\mathbf{B}_i)\mathbf{x}_{i+1-n} - (\mathbf{H}_{37}\mathbf{B}_{i+1} + \mathbf{H}_{38}\mathbf{B}_i)\mathbf{x}_{i-n} \end{bmatrix} \quad (42)$$

Combining Eqs. (3), (14), and (24), a discrete mapping can be obtained using 4th-4th HFDM as follow

$$\mathbf{x}_{i+1} = (\mathbf{I} - \mathbf{G}_{49}\mathbf{B}_{i+1} - \mathbf{G}_{410}\mathbf{B}_i) \begin{bmatrix} (\mathbf{G}_{47}\mathbf{B}_{i+1} + \mathbf{G}_{48}\mathbf{B}_i + \mathbf{F}_0)\mathbf{x}_i + (\mathbf{G}_{45}\mathbf{B}_{i+1} + \mathbf{G}_{46}\mathbf{B}_i)\mathbf{x}_{i-1} + \\ (\mathbf{G}_{43}\mathbf{B}_{i+1} + \mathbf{G}_{44}\mathbf{B}_i)\mathbf{x}_{i-2} + (\mathbf{G}_{41}\mathbf{B}_{i+1} + \mathbf{G}_{42}\mathbf{B}_i)\mathbf{x}_{i-3} - \\ (\mathbf{H}_{41}\mathbf{B}_{i+1} + \mathbf{H}_{42}\mathbf{B}_i)\mathbf{x}_{i+4-n} - (\mathbf{H}_{43}\mathbf{B}_{i+1} + \mathbf{H}_{44}\mathbf{B}_i)\mathbf{x}_{i+3-n} - \\ (\mathbf{H}_{45}\mathbf{B}_{i+1} + \mathbf{H}_{46}\mathbf{B}_i)\mathbf{x}_{i+2-n} - (\mathbf{H}_{47}\mathbf{B}_{i+1} + \mathbf{H}_{48}\mathbf{B}_i)\mathbf{x}_{i+1-n} \\ (\mathbf{H}_{49}\mathbf{B}_{i+1} + \mathbf{H}_{410}\mathbf{B}_i)\mathbf{x}_{i-n} \end{bmatrix} \quad (43)$$

References

- Altintas Y (2000) Manufacturing automation: metal cutting mechanics, machine tool vibrations, and CNC design. Cambridge University Press, Cambridge
- Altintas Y, Budak E (1995) Analytical prediction of stability lobes in milling. *CIRP Ann Manuf Technol* 44(1):357–362. [https://doi.org/10.1016/S0007-8506\(07\)62342-7](https://doi.org/10.1016/S0007-8506(07)62342-7)
- Merdol SD, Altintas Y (2004) Multi frequency solution of chatter stability for low immersion milling. *J Manuf Sci Eng* 126(3):459–466. <https://doi.org/10.1115/1.1765139>
- Balachandran B (2001) Nonlinear dynamics of milling processes. *Philos Trans R Soc A Math Phys Eng Sci* 359(1781):793–819. <https://doi.org/10.1098/rsta.2000.0755>
- Balachandran B, Gilsinn D (2005) Non-linear oscillations of milling. *Math Comp Model Dyn* 11(3):273–290. <https://doi.org/10.1080/13873950500076479>
- Long XH, Balachandran B, Mann BP (2007) Dynamics of milling processes with variable time delays. *Nonlinear Dyn* 47(1–3):49–63. <https://doi.org/10.1007/s11071-006-9058-4>
- Long XH, Balachandran B (2007) Stability analysis for milling process. *Nonlinear Dyn* 49:349–359. <https://doi.org/10.1007/s11071-006-9127-8>
- Bayly PV, Halley JE, Mann BP, Davies MA (2003) Stability of interrupted cutting by temporal finite element analysis. *J Manuf Sci Eng* 125(2):220–225. <https://doi.org/10.1115/1.1556860>
- Insperger T, Stépán G (2004) Updated semi-discretization method for periodic delay-differential equations with discrete delay. *Int J Numer Methods Eng* 61(1):117–141. <https://doi.org/10.1002/nme.1061>
- Insperger T, Stépán G, Turi J (2008) On the higher-order semi-discretizations for periodic delayed systems. *J Sound Vib* 313(1–2):334–341. <https://doi.org/10.1016/j.jsv.2007.11.040>
- Butcher EA, Bobrenkov OA, Bueler E, Nindujarla P (2009) Analysis of milling stability by the Chebyshev collocation method: algorithm and optimal stable immersion levels. *J Comput Nonlinear Dyn* 4(3):031003. <https://doi.org/10.1115/1.3124088>
- Ding Y, Zhu LM, Zhang XJ, Ding H (2010) A full-discretization method for prediction of milling stability. *Int J Mach Tools Manuf* 50(5):502–509. <https://doi.org/10.1016/j.ijmactools.2010.01.003>
- Ding Y, Zhu LM, Zhang XJ, Ding H (2011) Numerical integration method for prediction of milling stability. *J Manuf Sci Eng* 133(3):031005. <https://doi.org/10.1115/1.4004136>
- Ding Y, Zhu LM, Zhang XJ, Ding H (2013) Stability analysis of milling via the differential quadrature method. *J Manuf Sci E Trans ASME* 135(4):044502. <https://doi.org/10.1115/1.4024539>
- Li M, Zhang G, Huang Y (2013) Complete discretization scheme for milling stability prediction. *Nonlinear Dyn* 71:187–199. <https://doi.org/10.1007/s11071-012-0651-4>
- Niu JB, Ding Y, Zhu LM, Ding H (2014) Runge-Kutta methods for a semi-analytical prediction of milling stability. *Nonlinear Dyn* 76(1):289–304. <https://doi.org/10.1007/s11071-013-1127-x>
- Li Z, Yang Z, Peng Y, Zhu F, Ming X (2015) Prediction of chatter stability for milling process using Runge-Kutta-based complete discretization method. *Int J Adv Manuf Technol* 86(1):943–952. <https://doi.org/10.1007/s00170-015-8207-7>
- Xie QZ (2016) Milling stability prediction using an improved complete discretization method. *Int J Adv Manuf Technol* 83(5–8):815–821. <https://doi.org/10.1007/s00170-015-7626-9>
- Zhang Z, Li HG, Meng G, Liu C (2015) A novel approach for the prediction of the milling stability based on the Simpson method. *Int J Mach Tools Manuf* 99:43–47. <https://doi.org/10.1016/j.ijmactools.2015.09.002>
- Lehotzky D, Insperger T, Khasawneh F, Stepan G (2017) Spectral element method for stability analysis of milling processes with discontinuous time-periodicity. *Int J Adv Manuf Technol* 89(9–12):2503–2514. <https://doi.org/10.1007/s00170-016-9044-z>
- Zhang XJ, Xiong CH, Ding Y, Ding H (2017) Prediction of chatter stability in high speed milling using the numerical differentiation method. *Int J Adv Manuf Technol* 89(9–12):2535–2544. <https://doi.org/10.1007/s00170-016-8708-z>
- Qin CJ, Tao JF, Li L, Liu CL (2017) An Adams-Moulton-based method for stability prediction of milling processes. *Int J Adv Manuf Technol* 89(9–12):3049–3058. <https://doi.org/10.1007/s00170-016-9293-x>
- Jiang S, Sun Y, Yuan X, Liu W (2017) A second-order semi-discretization method for the efficient and accurate stability prediction of milling process. *Int J Adv Manuf Technol* 92(1–4):583–595. <https://doi.org/10.1007/s00170-017-0171-y>
- Li H, Dai Y, Fan Z (2019) Improved precise integration method for chatter stability prediction of two-DOF milling system. *Int J Adv Manuf Technol* 101(5–8):1235–1246. <https://doi.org/10.1007/s00170-018-2981-y>
- Ding Y, Zhu LM, Zhang XJ, Ding H (2010) Second-order full-discretization method for milling stability prediction. *Int J Mach Tools Manuf* 50(10):926–932. <https://doi.org/10.1016/j.ijmactools.2010.05.005>
- Liu YL, Zhang DH, Wu BH (2012) An efficient full-discretization method for prediction of milling stability. *Int J Mach Tools Manuf* 63:44–48. <https://doi.org/10.1016/j.ijmactools.2012.07.008>
- Guo Q, Sun YW, Jiang Y (2012) On the accurate calculation of milling stability limits using third-order full-discretization method. *Int J Mach Tools Manuf* 62:61–66. <https://doi.org/10.1016/j.ijmactools.2012.05.001>
- Ozoegwu CG (2014) Least squares approximated stability boundaries of milling process. *Int J Mach Tools Manuf* 79:24–30. <https://doi.org/10.1016/j.ijmactools.2014.02.001>
- Ozoegwu CG, Omenyi SN, Ofochebe SM (2015) Hyper-third order full-discretization methods in milling stability prediction. *Int J Mach Tools Manuf* 92:1–9. <https://doi.org/10.1016/j.ijmactools.2015.02.007>
- Ji YJ, Wang XB, Liu ZB, Wang HJ, Yan ZH (2018) An updated full-discretization milling stability prediction method based on the higher-order Hermite-Newton interpolation polynomial. *Int J Adv Manuf Technol* 95(5–8):2227–2242. <https://doi.org/10.1007/s00170-017-1409-4>
- Tang X, Peng F, Yan R, Gong Y, Li Y, Jiang L (2016) Accurate and efficient prediction of milling stability with updated full-discretization method. *Int J Adv Manuf Technol* 88(9–12):2357–2368. <https://doi.org/10.1007/s00170-016-8923-7>
- Yan ZH, Wang XB, Liu ZB, Wang DQ, Jiao L, Ji YJ (2017) Third-order updated full-discretization method for milling stability prediction. *Int J Adv Manuf Technol* 92(5–8):2299–2309. <https://doi.org/10.1007/s00170-017-0243-z>
- Zhou K, Feng P, Xu C, Zhang J, Wu Z (2017) High-order full-discretization methods for milling stability prediction by interpolating the delay term of time-delayed differential equations. *Int J Adv Manuf Technol* 93(5–8):2201–2214. <https://doi.org/10.1007/s00170-017-0692-4>

Publisher's note Springer Nature remains neutral with regard to jurisdictional claims in published maps and institutional affiliations.